Hybrid Materials

DOI: 10.1002/anie.200805773

# Incorporation of $Fe_3O_4$ Nanoparticles into Organometallic Coordination Polymers by Nanoparticle Surface Modification**

*Sang Bok Kim, Chen Cai, Shouheng Sun, and Dwight A. Sweigart**

Materials at the nanometer scale have been studied for decades because of unique properties arising from the large fraction of atoms residing on the surface. The size-dependent and shape-dependent physical and chemical properties of the nanoparticles (NPs) offer potential applications in catalysis, sensors, molecular electronics, and electrochemical biosensors.[1] Chemically synthesized magnetic NPs have drawn much attention, owing to unique magnetic properties derived from the small particle size and uniform size distribution.[1,2] Almost all magnetic NPs are superparamagnetic owing to their small size. Bulk superparamagnetic materials are intrinsically nonmagnetic but can be readily magnetized in the presence of an external magnetic field.[3,4] Among these magnetic materials, superparamagnetic iron oxide NPs with suitable biocompatible coatings have been used in biomedical applications such as magnetic resonance imaging (MRI) contrast enhancement, tissue engineering, and drug delivery.[5] Many chemical routes for the synthesis of NPs rely on varying the type and concentration of surfactants to tune the size of the NP. The resultant NPs are protected against oxidation and aggregation by a layer of surfactant molecules which make them soluble in nonpolar solvents and unstable in polar solvents. The polar head of the surfactant molecules adsorbs to the surface of the NPs, and the nonpolar tail of the surfactants is soluble in nonpolar solvents. To make nanoparticles soluble in polar solvents, two methods are commonly used. In the first, bilayer formation occurs when a long-chain polar surfactant interdigitates with the surfactant hydrocarbon tails around the nanoparticles and provides a positive surface charge. For example, dodecylamine-capped gold nanoparticles dispersed in chloroform have been transferred into water using cetyltrimethylammonium bromide.[6] The second method involves ligand exchange[3,7] by adding to the nanoparticle solution an excess of ligand which has a functional group, such as a thiol, that can displace the original ligand on the NP surface at one end and has a polar tail or polar functional group at the other end.[8,9]

Herein, we report that oleylamines on $Fe_3O_4$ NPs, with both oleylamine and oleic acid on the surface, can be replaced selectively by [($\eta^5$-semiquinone)$Mn(CO)_3$] (SQMTC). The resulting surface modified $Fe_3O_4$ NPs can subsequently function as a nucleus or template for the generation of crystalline coordination polymers that contain $Fe_3O_4$ NPs. The presence of $Fe_3O_4$ NPs allows for facile separation of the hybrid material by magnetic decantation. Hybridized magnetic properties can be obtained by introducing paramagnetic metal nodes, such as $Mn^{2+}$, into the coordination polymers.

The complex [($\eta^6$-hydroquinone)$Mn(CO)_3$]$BF_4$ (HQMTC; Scheme 1) underwent two deprotonations. The first deprotonation generated [($\eta^5$-semiquinone)$Mn(CO)_3$] (SQMC), which underwent a second deprotonation by reaction with metal acetates, such as $Mn(OAc)_2$ and $Cd(OAc)_2$. The resulting [($\eta^4$-quinone)$Mn(CO)_3$]$^-$ anion (QMTC) could then be used as the spacer in the formation of coordination polymers (Scheme 1).[10] Hence, SQMTC can be viewed as a precursor in the formation of coordination polymers. All three species, HQMTC, SQMTC, and QMTC, are stable in DMSO.

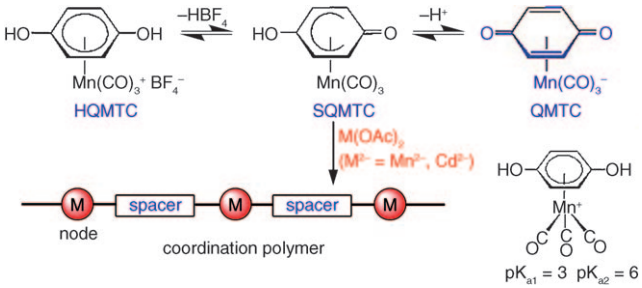


***Scheme 1.*** Deprotonation of [($\eta^6$-hydroquinone)$Mn(CO)_3$]$BF_4$ (HQMTC) and formation of coordination polymers with $Mn^{II}$ or $Cd^{II}$ nodes containing the organometallic ligand [($\eta^4$-quinone)$Mn(CO)_3$]$^-$ (QMTC) as the spacer.

Surface modification of $Fe_3O_4$ NPs was carried out by exchanging the surface oleylamine species with SQMTC. To accomplish this modification, Solutions of $Fe_3O_4$ NPs in hexane and HQMTC in DMSO were combined in a vial and shaken. The $Fe_3O_4$ NPs were transferred from the hexane layer to the DMSO layer (Scheme 2). When [($\eta^6$-1,4-dimethoxybenzene)$Mn(CO)_3$]$BF_4$ was used instead of HQMTC, there was no NP transfer to the DMSO solution.

The obvious conclusion from this observation is that the ability of HQMTC to function as a moderate-strength acid is responsible for the transfer. We postulate that HQMTC protonates the oleylamine, and that the resulting SQMTC and DMSO solvent take the place of the oleylamine on the NP surface. The resulting oleylammonium salts, which are

[*] S. B. Kim, C. Cai, Prof. S. Sun, Prof. D. A. Sweigart
Department of Chemistry, Brown University
Providence, RI 02912 (USA)
Fax: (+1) 401-863-9046
E-mail: dwight_sweigart@brown.edu

[**] We are grateful to the donors of the Petroleum Fund, administered by the American Chemical Society, and to the National Science Foundation (CHE-0308640) for support of this research.

Supporting information for this article is available on the WWW under http://dx.doi.org/10.1002/anie.200805773.

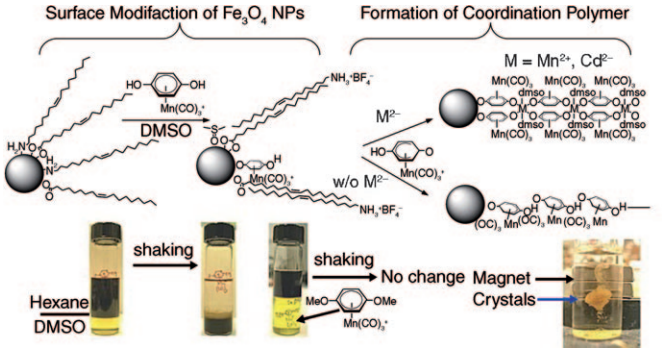


***Scheme 2.*** Surface modification of $Fe_3O_4$ NPs with binding of SQMTC, which serves as a template for the subsequent formation of coordination or H-bonded polymers.

liberated from the surface of the $Fe_3O_4$ NP, likely form a bilayer with the surface oleic acid groups. FT-IR spectra showed peaks corresponding to Fe–O groups in the $Fe_3O_4$ NPs themselves ($\tilde{\nu} = 587\ cm^{-1}$),[11] and the carbonyl ligands of SQMTC ($\tilde{\nu} = 2047, 1977\ cm^{-1}$; see the Supporting Information, Figure S1). Peaks corresponding to manganese in the energy-dispersive X-ray (EDS) spectrum confirmed the existence of SQMTC (see the Supporting Information, Figure S2).

Incorporation of $Fe_3O_4$ NPs (see the Supporting Information, Figure S3) into a polymer by a self-assembly process was accomplished by adding the surface-modified NPs to a solution of free SQMTC alone, or with $Mn(OAc)_2$ or $Cd(OAc)_2$, in DMSO. Crystals of both $[\{Mn(QMTC)_2(dmso)_2\}_n]$–$Fe_3O_4$ NP (Figure 1a) and $[(SQMTC)_n]$–$Fe_3O_4$ NP (Figure 1d) started to grow within ten minutes. The $[\{Cd(QMTC)_2(dmso)_2\}_n]$–$Fe_3O_4$ NP crystals were grown at room temperature overnight (Figure 2a, b, and Figure S4 in the Supporting Information). The crystals were separated by magnetic decantation and washed with fresh DMSO and

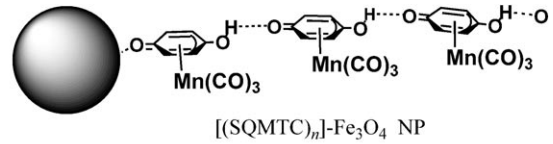


$[(SQMTC)_n]$-$Fe_3O_4$ NP

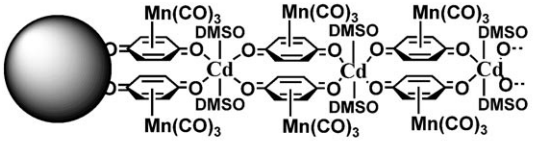


$[\{Cd(QMTC)_2(dmso)_2\}_n]$-$Fe_3O_4$ NP

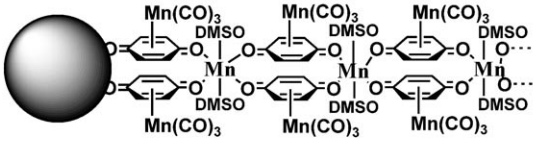


$[\{Mn(QMTC)_2(dmso)_2\}_n]$-$Fe_3O_4$ NP

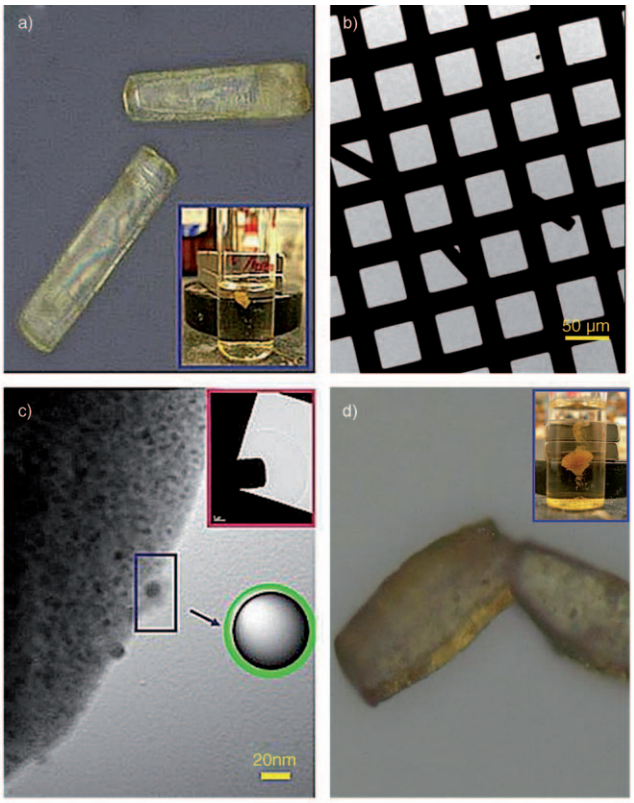


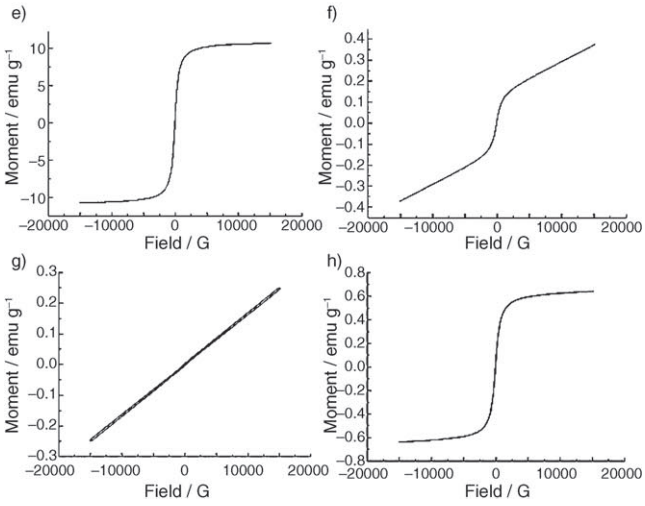


***Figure 1.*** a) Optical microscope image of $[\{Mn(QMTC)_2(dmso)_2\}_n]$–$Fe_3O_4$ NP crystals; b) TEM image of $[\{Mn(QMTC)_2(dmso)_2\}_n]$–$Fe_3O_4$ NP crystals (see Scheme 1) on TEM grid; c) TEM image of a $Fe_3O_4$ NP with a shell of $[\{Mn(QMTC)_2(dmso)_2\}_n]$–$Fe_3O_4$ NP crystal; d) optical microscope image of $[(SQMTC)_n]$–$Fe_3O_4$ NP crystal (see Scheme 1); e) magnetization curve of $Fe_3O_4$ NP; f) magnetization curve of $[\{Mn(QMTC)_2(dmso)_2\}_n]$–$Fe_3O_4$ NP crystal; g) magnetization curve of $[\{Mn(QMTC)_2(dmso)_2\}_n]$ crystal; h) magnetization curve of $[(SQMTC)_n]$–$Fe_3O_4$ NP crystal.

acetone (Scheme 2). FT-IR spectra of $[(SQMTC)_n]$–$Fe_3O_4$ NP and $[\{M(QMTC)_2(dmso)_2\}_n]$–$Fe_3O_4$ NP (M = Mn, Cd) correlate well with the reported values of the respective polymer without the presence of NP (see the Supporting Information, Figure S5).[9a,13] Inductively coupled plasma

  

atomic emission spectrophotometry (ICP-AES) analyses indicated 1.02 wt.% of Fe in $[(SQMTC)_n]$–$Fe_3O_4$ NP crystals and 0.82 wt.% of Fe in $[\{Mn(QMTC)_2(dmso)_2\}_n]$–$Fe_3O_4$ NP crystals. For $[\{Cd(QMTC)_2(dmso)_2\}_n]$–$Fe_3O_4$ NP, EDS confirmed the presence of Mn from SQMTC, Cd from the metal nodes, and Fe from $Fe_3O_4$ NPs (see the Supporting Information, Figure S6). ICP-AES analysis showed 1.97 wt.% of Fe in the crystal.

Crystals of both $[\{M(QMTC)_2(dmso)_2\}_n]$–$Fe_3O_4$ NP (M = Mn, Cd) and $[(SQMTC)_n]$–$Fe_3O_4$ NP were attracted to a magnet (Figure 1a, d, 2d), implying the existence of superparamagnetic $Fe_3O_4$ NPs. The distribution of $Fe_3O_4$ NPs inside the crystal could not be observed by TEM as a result of the thickness of the crystals (Figure 1b). $Fe_3O_4$ NPs could only be visualized at the edge of the $[\{Mn(QMTC)_2(dmso)_2\}_n]$–$Fe_3O_4$ NP crystal (Figure 1c). The $Fe_3O_4$ NP on the edge of the crystal has an organometallic shell, which we postulated to be $[\{Mn(QMTC)_2(dmso)_2\}_n]$[1a] on the surface of the modified $Fe_3O_4$ NP. This assumption was confirmed by single-crystal X-ray diffraction of the crystals in Figure 1a. The solved structure matched a known $[Mn(QMTC)_2(dmso)_2]$ structure.[10] Visible aggregates of $Fe_3O_4$ NPs in the $[\{Mn(QMTC)_2(dmso)_2\}_n]$–$Fe_3O_4$ NP crystals could not be observed by an optical microscope (Figure 1a).

The isolated crystals of $[\{Cd(QMTC)_2(dmso)_2\}_n]$–$Fe_3O_4$ NP were redispersed in fresh DMSO, dropped onto a TEM grid, and dried under nitrogen. The resultant TEM image shows that the $Fe_3O_4$ NPs are aggregated (Figure 2c). As in the case of $[\{Mn(QMTC)_2(dmso)_2\}_n]$–$Fe_3O_4$ NP (Figure 1c), the $Fe_3O_4$ NPs have organometallic shells, which are formed by coordination polymerization of $Cd^{2+}$ ions and QMTC groups on the surface of the surface-modified $Fe_3O_4$ NP. In the middle of the crystal of $[\{Cd(QMTC)_2(dmso)_2\}_n]$–$Fe_3O_4$ NP, aggregates of $Fe_3O_4$ NPs are seen as brown spots (Figure 2a, b). Single-crystal X-ray diffraction verified that $[\{Cd(QMTC)_2(dmso)_2\}_n]$–$Fe_3O_4$ NP consisted of the postulated coordination polymer.

Crystals of $[(SQMTC)_n]$–$Fe_3O_4$ NP (Figure 1d) feature hydrogen bonds between SQMTC organometallic molecules. The ability of the SQMTC molecule to bind to Fe on the NP surface through the C=O group and simultaneously present an OH group to form a hydrogen bond to excess SQMTC accounts for the resultant polymer formation. The magnetic properties of $[\{Mn(QMTC)_2(dmso)_2\}_n]$–$Fe_3O_4$ NP, $[(SQMTC)_n]$–$Fe_3O_4$ NP and $[\{Cd(QMTC)_2(dmso)_2\}_n]$–$Fe_3O_4$ NP were determined by the use of a vibrational sample magnetometer (VSM). Both SQMTC and QMTC are diamagnetic. When QMTC (spacer) coordinates to $Mn^{2+}$ (metal node), paramagnetic metal ions are incorporated into the polymer. The magnetization curve of pure $[\{Mn(QMTC)_2(dmso)_2\}_n]$ crystals (Figure 1g) shows that it follows simple paramagnetic behavior. The same material grown in the presence of NPs exhibit superparamagnetic character in the approximate range of −2500 G to +2500 G and simple paramagnetic character (no magnetic saturation) in fields below about −2500 G and above 2500 G (Figure 1f). The magnetization curve of the $[(SQMTC)_n]$–$Fe_3O_4$ NP crystals (Figure 1h) shows that it has simple superparamagnetic character, which arises from the incorporated $Fe_3O_4$ NPs.

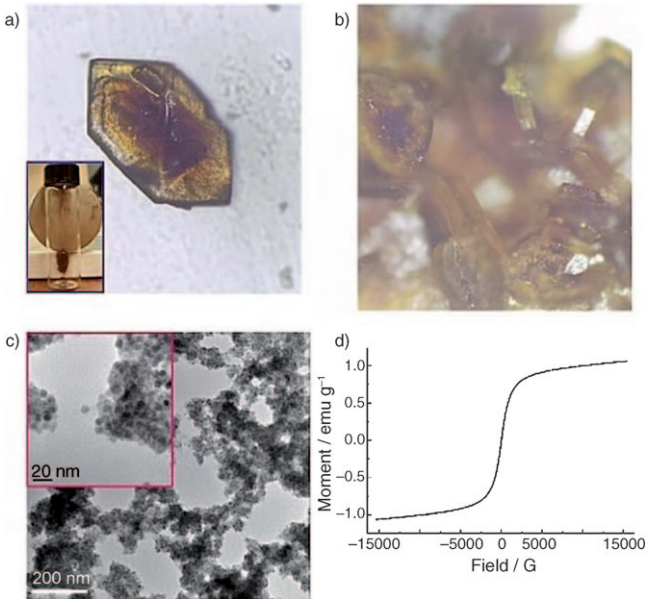


***Figure 2.*** a) Optical microscope image of a $[\{Cd(QMTC)_2(dmso)_2\}_n]$–$Fe_3O_4$ NP crystal; b) enlarged optical microscopic image of $[\{Cd(QMTC)_2(dmso)_2\}_n]$–$Fe_3O_4$ NP crystal; c) TEM image of the aggregated $Fe_3O_4$ NPs which have an organometallic coordination polymer shell formed during the crystallization process; d) magnetization curve for $[\{Cd(QMTC)_2(dmso)_2\}_n]$–$Fe_3O_4$ NP crystal.

Similar behavior is exhibited by $[\{Cd(QMTC)_2(dmso)_2\}_n]$–$Fe_3O_4$ NP (Figure 2d).

Crystals of $[\{Mn(QMTC)_2(dmso)_2\}_n]$–$Fe_3O_4$ NP were obtained in ten minutes, whereas those of $[\{Cd(QMTC)_2(dmso)_2\}_n]$–$Fe_3O_4$ NP were grown more slowly (overnight). In the optical microscopic image of $[\{Cd(QMTC)_2(dmso)_2\}_n]$–$Fe_3O_4$ NP, $Fe_3O_4$ NPs can be seen as an aggregate in the middle of the coordination polymer crystal (Figure 2a, b). $Fe_3O_4$ NPs can not be seen in $[\{Mn(QMTC)_2(dmso)_2\}_n]$–$Fe_3O_4$ NP crystals in the optical microscopic image (Figure 1a), suggesting a more uniform dispersion in the $Mn^{II}$ polymer compared to the $Cd^{II}$ analogue.

In summary, oleylamines on the surface of $Fe_3O_4$ NPs, incorporating both oleylamine and oleic acid as surfactants, can be replaced selectively by SQMTC. The modified $Fe_3O_4$ NPs are soluble in DMSO. Organometallic coordination polymerization on the surface-modified $Fe_3O_4$ NPs in DMSO allowed the incorporation of $Fe_3O_4$ NPs into organometallic coordination polymers. We prepared hybrid materials containing superparamagnetic $Fe_3O_4$ NPs and either paramagnetic $Mn^{II}$ or diamagnetic $Cd^{II}$ as nodes. The incorporation of nanosized functional materials into the coordination polymers may generate a large number of applications.[14]

## *Experimental Section*

Surface modification of $Fe_3O_4$ NPs: A solution of as-made $Fe_3O_4$ NPs (ca. 20 mg) in hexane (2 mL) was mixed with $[(\eta^6\text{-hydroquinone})Mn(CO)_3]BF_4$ (40 mg, 0.12 mmol) in DMSO (2 mL). The mixed solution formed two layers, the upper (hexane) layer containing $Fe_3O_4$ NPs and the lower (DMSO) layer the organometallic complex.

  

After shaking for 3 h, all nanoparticles had transferred to the DMSO layer. To isolate the surface-modified NPs from the excess organometallic complex used in this process, the DMSO solution was mixed with excess fresh THF. The precipitated NPs were collected by a magnet, washed with fresh THF, and dried under vacuum for FT-IR analysis. The NPs were soluble in polar solvents, such as DMSO and acetone, and insoluble in comparatively nonpolar solvents, such as THF, dichloromethane, and hexane.

$[\{M(QMTC)_2(dmso)_2\}_n]$–$Fe_3O_4$ NP (M = Mn, Cd): A solution of $[(\eta^5\text{-semiquinone})Mn(CO)_3]$ (100 mg, 0.41 mmol) and manganese(II) acetate tetrahydrate (50 mg, 0.21 mmol) or cadmium(II) acetate trihydrate (60 mg, 0.21 mmol) in DMSO (5 mL) was heated to ensure complete dissolution, and allowed to cool to room temperature. As soon as the reaction mixture had cooled, a solution of $Fe_3O_4$ NPs, partially ligand-exchanged with $[(\eta^5\text{-semiquinone})Mn(CO)_3]$ (30 mg) in DMSO (2 mL) was added to it prior to crystallization. The resulting crystals were isolated by magnetic decantation and washed with fresh DMSO ($3 \times 10$ mL) and acetone (10 mL). The procedure for $[(SQMTC)_n]$–$Fe_3O_4$ NP was the same as that for $[\{M(QMTC)_2(dmso)_2\}_n]$–$Fe_3O_4$ NP, except that no metal ($Mn^{2+}$ or $Cd^{2+}$) acetate was added.

Received: November 27, 2008
Published online: March 13, 2009

**Keywords:** coordination polymers · magnetic properties · nanoparticles · organic–inorganic hybrid composites · surfactants

[1] A. Merkoçi, *FEBS J.* **2007**, *274*, 310 – 316.
[2] V. Salgueiriño-Maceira, L. M. Liz-Marzán, M. Farle, *Langmuir* **2004**, *20*, 6946 – 6950.
[3] H. G. Bagaria, E. T. Ada, M. Shamsuzzoha, D. E. Nikles, D. T. Johnson, *Langmuir* **2006**, *22*, 7732 – 7737.
[4] A. Hu, G. T. Yee, W. Lin, *J. Am. Chem. Soc.* **2005**, *127*, 12486 – 12487.
[5] T. Yang, C. Shen, Z. Li, H. Zhang, C. Xiao, S. Chen, Z. Xu, D. Shi, J. Li, H. Gao, *J. Chem. Phys. B* **2005**, *109*, 23233 – 23236.
[6] A. Swami, A. Kumar, M. Sastry, *Langmuir* **2003**, *19*, 1168 – 1172.
[7] F. Dubois, B. Mahler, B. Dubertret, E. Doris, C. Mioskowski, *J. Am. Chem. Soc.* **2007**, *129*, 482 – 483.
[8] J. S. Choi, Y. W. Jun, S.-I. Yeon, H. C. Kim, J.-S. Shin, J. Cheon, *J. Am. Chem. Soc.* **2006**, *128*, 15982 – 15983.
[9] R. De Palma, S. Peeters, M. J. Van Bael, H. Van den Rul, K. Bonroy, W. Laureyn, J. Mullens, G. Borghs, G. Maes, *Chem. Mater.* **2007**, *19*, 1821 – 1831.
[10] a) M. Oh, G. B. Carpenter, D. A. Sweigart, *Angew. Chem.* **2001**, *113*, 3291 – 3294; *Angew. Chem. Int. Ed.* **2001**, *40*, 3191 – 3194; b) M. Oh, G. B. Carpenter, D. A. Sweigart, *Angew. Chem.* **2002**, *114*, 3802 – 3805; *Angew. Chem. Int. Ed.* **2002**, *41*, 3650 – 3653; c) M. Oh, G. B. Carpenter, D. A. Sweigart, *Angew. Chem.* **2003**, *115*, 2072 – 2074; *Angew. Chem. Int. Ed.* **2003**, *42*, 2026 – 2028; d) M. Oh, G. B. Carpenter, D. A. Sweigart, *Acc. Chem. Res.* **2004**, *37*, 1 – 11.
[11] a) M. Klokkenburg, J. Hilhorst, B. H. Erné, *Vib. Spectrosc.* **2007**, *43*, 243 – 248; b) Q. Lan, C. Liu, F. Yang, S. Liu, J. Xu, D. Sun, *J. Colloid Interface Sci.* **2007**, *310*, 260 – 269.
[12] M. Oh, G. B. Carpenter, D. A. Sweigart, *Organometallics* **2003**, *22*, 1437 – 1442.
[13] M. Oh, G. B. Carpenter, D. A. Sweigart, *Organometallics* **2002**, *21*, 1290 – 1295.
[14] a) M. Oh, C. A. Mirkin, *Nature* **2005**, *438*, 651 – 654; b) W. J. Rieter, K. M. Taylor, H. An, W. Lin, *J. Am. Chem. Soc.* **2006**, *128*, 9024 – 9025; c) I. Imaz, D. Maspoch, C. Rodriquez-Blanco, J. M. Perez-Falcon, J. Campo, D. Ruiz-Molina, *Angew. Chem.* **2008**, *120*, 1883 – 1886; *Angew. Chem. Int. Ed.* **2008**, *47*, 1857 – 1860; d) W. J. Rieter, K. M. Taylor, H. An, W. Lin, *J. Am. Chem. Soc.* **2007**, *129*, 9852 – 9853.

  